Removal of NO in NO/N_2, $NO/N_2/O_2$, $NO/CH_4/N_2$, and $NO/CH_4/O_2/N_2$ Systems by Flowing Microwave Discharges

José L. Hueso,[†] Agustín R. González-Elipe,[†] José Cotrino,*[,†,‡] and Alfonso Caballero[†,§]

Instituto de Ciencia de Materiales de Sevilla (CSIC-Universidad de Sevilla), Avda Américo Vespucio 49, 41092 Sevilla, Spain, and Departamento de Química Inorgánica, Facultad de Química, and Departamento de Física Atómica, Molecular y Nuclear, Universidad de Sevilla, 41092 Sevilla, Spain

Received: May 29, 2006; In Final Form: October 31, 2006

In this paper, continuing previous work, we report on experiments carried out to investigate the removal of NO from simulated flue gas in nonthermal plasmas. The plasma-induced decomposition of small concentrations of NO in N_2 used as the carrier gas and O_2 and CH_4 as minority components has been studied in a surface wave discharge induced with a surfatron launcher. The reaction products and efficiency have been monitored by mass spectrometry as a function of the composition of the mixture. NO is effectively decomposed into N_2 and O_2 even in the presence of O_2, provided always that enough CH_4 is also present in the mixture. Other majority products of the plasma reactions under these conditions are NH_3, CO, and H_2. In the absence of O_2, decomposition of NO also occurs, although in that case HCN accompanies the other reaction products as a majority component. The plasma for the different reaction mixtures has been characterized by optical emission spectroscopy. Intermediate excited species of NO^*, C^*, CN^*, NH^*, and CH^* have been monitored depending on the gas mixture. The type of species detected and their evolution with the gas composition are in agreement with the reaction products detected in each case. The observations by mass spectrometry and optical emission spectroscopy are in agreement with the kinetic reaction models available in literature for simple plasma reactions in simple reaction mixtures.

I. Introduction

During the last years, nonthermal plasma procedures have been presented as a competitive technology for air cleaning and now it is clear that the reduction of pollutants from industrial processes and vehicle exhausts is one of the critical and urgent topics in environmental and pollution control research. Removal of NO from gas streams is one of the most challenging problems in this context. Its removal has been intended by means of different plasma procedures including barrier discharge plasmas (DBD),[1−5] corona discharges,[2,5−9] microwave plasmas (MW),[10−12] ac plasmas,[13] and hollow cathode plasmas.[14] As a general rule, in DBD discharges the presence of oxygen tends to produce the oxidation of NO to NO_2,[5,6] while in MW discharges dissociation of NO into N_2 and O_2 usually occurs.[15,16]

Many works in the literature dealing with this subject aim at describing the decomposition and/or reaction mechanisms of simple mixtures of NO with inert carrier gases or air.[2,4,5,13,17,18] Fewer works have addressed the fundamental problems involved during the removal of NO from complex mixtures as those existing in real combustion exhausts.[19,20] For example, gases produced by diesel engines and other combustion processes are a complex mixture of N_2 (majority component), remaining oxygen, CO_2, unburned hydrocarbons, water vapor, and soot particles in suspension.[21,22] The plasma chemistry of such complex mixtures is not easy, and its description and eventual optimization for NO removal requires a thorough assessment of the influence of the different plasma parameters (e.g., electric field frequency, microwave power, gas pressure, gas flow, reactor geometry, etc.) and a specific evaluation of the influence of the elemental reaction processes involved.

Flowing discharges containing nitrogen oxide have been the subject of different studies during the last years. Thus, the study of the kinetics of NO_x (i.e., NO + NO_2) in spatially homogeneous dc low-pressure discharges has been performed both theoretically and experimentally by Gordiets et al.[23] Similar reactions and the related kinetic models for flowing microwave discharges and postdischarges in N_2/O_2 mixtures have also raised much interest in the context of plasma sterilization processes and other industrial applications.[24−26] From these studies, for pressures above approximately 1 Torr and for values of reduced electric field strength (i.e., $E/N \sim 8 \times 10^{-16}$ V cm^2), a relatively high dissociation yield of NO should be expected in nitrogen glow discharges.[27] On the other hand, the decomposition of methane in nitrogen discharges has been the subject of numerous studies of interest in fields such as detoxification, atmospheric chemistry, synthesis, metal nitriding, etc.[28−30] From these and other studies, the kinetics of the methane decomposition in nitrogen plasmas has been established and the main dissociation mechanisms of CH_4 in a N_2/CH_4 mixtures have been proposed.[29−31] However, similar fundamental studies with more complex plasma mixtures are still scarce.[32] In this context, in a previous work using a surface wave (SW) setup and Ar as the carrier gas we have studied the MW plasma chemistry of complex mixtures of NO with other minority components such as hydrocarbons, oxygen, or nitrogen.[15] A 90% amount of NO removal can be achieved with mixtures of $Ar/NO/O_2/CH_4$. The addition of low amounts of N_2 and O_2 produced a decrease in

* To whom correspondence should be addressed. Fax: +34 954460665. E-mail: cotrino@us.es.

† Instituto de Ciencia de Materiales de Sevilla (Centro Mixto CSIC-Universidad de Sevilla).

‡ Departamento de Física Atómica, Molecular y Nuclear, Universidad de Sevilla.

§ Departamento de Química Inorgánica, Universidad de Sevilla.

10.1021/jp063315v CCC: $37.00
Published on Web 01/18/2007

TABLE 1: Reaction Products for $N_2 + O_2 + NO$ Mixtures Containing Different Concentrations of O_2

reacn mixture	NO decomposn (%)	reacn products
$N_2 + NO$	97	N_2, O_2, N_2O (traces)
$N_2 + NO + O_2$ (1%)	95	N_2, O_2, N_2O (traces)
$N_2 + NO + O_2$ (3%)	70	N_2, O_2, NO, N_2O (traces)
$N_2 + NO + O_2$ (5%)	40	N_2, NO, N_2O (traces)

the decomposition yield, a feature that suggests that even smaller yields of decomposition might be obtained if N_2 is used as carrier gas. To address this question, in this work we have studied similar reactions by substituting Ar by N_2 as carrier gas. This experimental situation is closer to that existing in real exhausts, and therefore, the extrapolation of the obtained results to real working conditions could be more straightforward. As in the previous work using Ar as the carrier gas, here we have analyzed the different reaction products by mass spectrometry (MS) and identified intermediate species in the plasma by optical emission spectroscopy (OES). The obtained results have evidenced that the decomposition of NO into N_2 and O_2 is very high even in the presence of oxygen, provided that CH_4 is added to the reaction mixture. Plasma reactors require a very complex modeling because of the self-consistent coupling of the fluid dynamics, electrodynamics phenomena, and reaction kinetics. In this work, we have mainly focused on the chemical mechanisms trying to account for the removal of NO as a result of chemical reactions in the nonthermal plasma phase. For this purpose, we have considered the kinetic data available in the literature for simple reactions, involving radicals and excited species. Thus, these reactions provide a comprehensive description of more complex reaction processes taking place under our experimental conditions.

II. Experimental Section

A scheme of the experimental setup is reported in a previous work.[15] The plasma reactor consists of a quartz tube of 3.5 mm inner diameter. The plasma is produced by a 2.45 GHz surfatron exciter. Microwave power is transported from the power supply to the surfatron via a coaxial cable coupled with a slot antenna directly connected to the launcher. A power of 60 W was used in the experiments. Although this parameter was not modified for the series of experiments reported here, it is worth noting that very similar results were also obtained for smaller powers down to 20 mW, a value at which the plasma already extinguished. The traveling microwave power and the electron density decrease from the excitation gap to the plasma end, where the electron density reaches its critical value (approximately 3.7×10^{11} cm^{-3} at 2450 MHz). The gas mixtures were prepared with mass flow controllers connected to the entrance of the quartz tube. The mass flow of N_2 used as carrier gas was fixed at 25 sccm. Typical compositions of gas mixtures were as follows: NO (3000 ppm); O_2 (from 0 to 5% in volume); CH_4 (from 0 to 5000 ppm). The total pressure in the reactor was controlled by adjusting a throttle valve placed between the reactor and a vacuum pump. Experiments were carried out for different compositions of the gas mixtures around the aforementioned values and a total pressure of 45 torrs. This parameter was maintained fixed in all the experiments since no significant changes in reaction efficiency were observed between 30 and 75 torrs. Plasma extends over a few centimetres and is followed by a homogeneous afterglow along the postdischarge. Analysis of the gas mixtures before and after plasma ignition was done by mass spectrometry (MS) (QMS 422 from Balzers). The gases were sampled to the mass spectrometer through a calibrated leak valve. When possible, calibration of the peak intensities is carried out with simple mixtures of N_2 with either the reactants or the gases obtained as products of the reactions. The accuracy of the analysis is considered to be within 12% of maximum uncertainty. The induction period to reach steady-state conditions was very small, in any case shorter than 10 s.

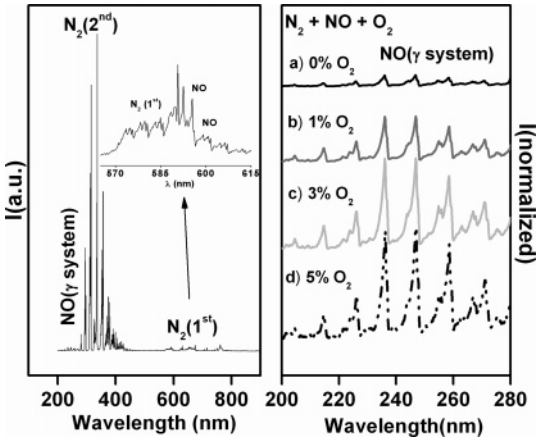

Figure 1. Left: Wide scan OES spectrum of a $N_2 + O_2 + NO$ mixture. The inset shows in an enlarged scale the bands due to the first positive N_2 system and the NO bands first reported by Tanaka et al.[33] Right: Series of spectra for the zone comprised between 200 and 280 nm corresponding to the vibrational bands of NO* species for different concentrations of O_2. The intensity of the bands has been normalized to the intensity of the N_2^* peak at 337.13 nm.

Study of the plasma by OES is carried out by collecting the light with an optical fiber and analyzing the emitted spectra with a Jobin Ybon (HR250) scanning monochromator and a Hamamatsu photomultiplier tube (R928). The whole system was operated and the signals were collected with a personal computer.

III. Results

A. Mixtures N_2/NO and N_2/NO/O_2. The plasma activation in the SW reactor of a N_2/NO mixture yields O_2 as majority detectable product with a NO decomposition efficiency of 97% as reported in Table 1. An equivalent amount of N_2 is supposed to be formed, although its determination by MS was not possible because this product is also the carrier gas. This result indicates that even in the presence of a high concentration of N_2, the NO is effectively dissociated by a flowing SW plasma excitation. By MS analysis it is also possible to detect the formation of traces of N_2O as a minority product. As reported in Table 1, the addition of O_2 to the reaction mixture produces a decrease in the efficiency of the process that reaches only a 40% NO dissociation for a concentration of 5% oxygen and of 70% for 3% oxygen. This dissociation yield is higher than the 42% found previously in a SW discharge for $Ar + N_2$ (3%) + O_2 (3%) + NO mixtures.[15]

Interesting hints about the reaction mechanism can be obtained by the OES detection of the intermediate species of the plasma. Figure 1 (left) shows a wide scan spectrum comprising the main bands found for the N_2/O_2/NO system. The bands of the second positive system of N_2 (bands from 280 to 497 nm, $N_2(C^3\Pi_u, v' = 4 \rightarrow N_2(B^3\Pi_g, v'' = 4) + h\nu$, at 326.8 nm)[33] are relatively more intense than the others. Therefore, these bands are used for the normalization of the OES spectra. The bands of the nitrogen first positive system ($N_2(B^3\Pi_g, v' = 6 \rightarrow N_2(A^3\Sigma_u^+, v'' = 1) + h\nu$, at 662.3 nm) present a smaller intensity and are also depicted in an enlarged scale in that figure. The NOγ system, produced by radiative decay of NO($A^2\Sigma^+$)

TABLE 2: Summary and Attribution of the Main Bands Detected by OES for the Different Gas Mixtures

reacn mixture	species (system)	electronic transitions	peaks and bands intervals
$N_2 + NO + O_2$	N_2 (2nd positive system)	$C\ ^3\Pi \rightarrow B\ ^3\Pi$	281.43−497.64
	N_2 (1st positive system)	$B\ ^3\Pi \rightarrow A^3\Sigma$	503.08−10420
	NO (γ system)	$A^2\Sigma^+ \rightarrow {}^2\Pi$	195.61−345.85
	N_2^+ (main system)	$^2\Sigma \rightarrow {}^2\Sigma$	329.34−586.47
	NO (Tanaka et al.)		523.22−642.94
$N_2 + NO + CH_4$	N_2 (2nd positive system)	$C\ ^3\Pi \rightarrow B\ ^3\Pi$	281.43−497.64
	N_2 (1st positive system)	$B\ ^3\Pi \rightarrow A\ ^3\Sigma$	503.08−10420
	NO (γ system)	$A\ ^2\Sigma^+ \rightarrow {}^2\Pi$	195.61−345.85
	N_2^+ (main system)	$^2\Sigma \rightarrow {}^2\Sigma$	329.34−586.47
	NO (Tanaka et al.)		523.22−642.94
	NH (3360 A system)	$^3\Pi \rightarrow {}^3\Sigma$	336.00−337.00
	CN (violet system)	$^2\Sigma \rightarrow {}^2\Sigma$	358.59−460.61
	CN (red system)	$^3\Pi \rightarrow {}^2\Sigma$	437.38−939.30
	CH (A 4300 system)	$^2\Delta \rightarrow {}^2\Pi$	431.25−494.00
	N I	$^4P^\circ \rightarrow {}^4P$	672.09
	C I	$^1S \rightarrow {}^1P^\circ$	247.86
	H	$^1P^\circ \rightarrow {}^2D$	656.28
$N_2 + CH_4 + O_2$	N_2 (2nd positive system)	$C\ ^3\Pi \rightarrow B\ ^3\Pi$	281.43−497.64
	N_2 (1st positive system)	$B\ ^3\Pi \rightarrow A\ ^3\Sigma$	503.08−10420
	NO (γ system)	$A\ ^2\Sigma^+ \rightarrow {}^2\Pi$	195.61−345.85
	N_2^+ (main system)	$^2\Sigma \rightarrow {}^2\Sigma$	329.34−586.47
	NH (3360 A system)	$^3\Pi \rightarrow {}^3\Sigma$	336.00−337.00
	CN (violet system)	$^2\Sigma \rightarrow {}^2\Sigma$	358.59−460.61
	CN (red system)	$^3\Pi \rightarrow {}^2\Sigma$	437.38−939.30
	CH (A 4300 system)	$^2\Delta \rightarrow {}^2\Pi$	431.25−494.00
	N I	$^4P^\circ \rightarrow {}^4P$	672.09
	C I	$^1S \rightarrow {}^1P^\circ$	247.86
	H	$^1P^\circ \rightarrow {}^2D$	656.28; 486.13
$N_2 + CH_4 + O_2 + NO$	N_2 (2nd positive system)	$C\ ^3\Pi \rightarrow B\ ^3\Pi$	281.43−497.64
	N_2 (1st positive system)	$B\ ^3\Pi \rightarrow A\ ^3\Sigma$	503.08−10420
	N_2^+ (main system)	$^2\Sigma \rightarrow {}^2\Sigma$	329.34−586.47
	NO (γ system)	$A\ ^2\Sigma^+ \rightarrow {}^2\Pi$	195.61−345.85
	NH (3360 A system)	$^3\Pi \rightarrow {}^3\Sigma$	336.00−337.00
	CN (violet system)	$^2\Sigma \rightarrow {}^2\Sigma$	358.59−460.61
	N I	$^4P^\circ \rightarrow {}^4P$	672.09
	H	$^1P^\circ \rightarrow {}^2D$	656.28

TABLE 3: Reaction Products for $N_2 + CH_4 + O_2$ Mixtures Containing Different Concentrations of O_2

reacn mixture	O_2 conversn (%)	CH_4 removal (%)	reacn products (ppm)
$N_2 + CH_4$		100	H_2, HCN (<3000), NH_3 (<3000), H_2O[a] (traces)
$N_2 + CH_4 + O_2$ (0.3%)	98	100	H_2, NH_3 (<500), H_2O (<4500), CO (<1600), HCN (<1400)
$N_2 + CH_4 + O_2$ (1%)	65	100	H_2, NH_3, H_2O (<8400), CO (<2900), N_2O (<300)
$N_2 + CH_4 + O_2$ (3%)	28	100	H_2, NH_3, CO (<2000), H_2O (<8000), CO_2 (<400), N_2O (traces), NO (traces)

[a] H_2O from humidity on the walls of the reactor

excited states, is detected at 247.9 nm. By contrast, NOβ emission bands are not observed in our system.[33] It is also interesting the appearance of some peculiar bands in the range 523−643 nm which have been assigned to NO^* (i.e., excited NO) by other authors (Tanaka et al. and Grillet et al.).[33] Figure 1 (right) shows different spectra of the NO γ system corresponding to the vibrational structure of NO^* species detected in the range 200−280 nm for $N_2 + NO$ and $N_2 + O_2 + NO$ mixtures with different concentrations of O_2. This figure shows that the intensity of the NO^* bands increases as the amount of O_2 in the mixture increases. A summary of the assignments of the different bands and peaks detected under the different conditions explored in this work is presented in Table 2.

B. N_2/CH_4 and $N_2/CH_4/O_2$ Mixtures. Real exhaust mixtures coming from diesel and other combustion processes contain, among other components, unburned hydrocarbons. Therefore, it is pertinent to study the plasma reactions of hydrocarbons and oxygen as minority components and N_2 as carrier gas as a preliminary step prior to the consideration of complex mixtures containing NO. Table 3 summarizes the main products of the plasma reactions detected by MS analysis for mixtures with three different concentrations of oxygen.

In all cases, CH_4 reacts almost completely (i.e., decomposition yield higher than 99%). This indicates that oxygen is used to burn the methane. For the N_2/CH_4 mixture without oxygen, the products of the reaction are HCN, H_2, and NH_3 plus some traces of H_2O from the inner walls of the reactor. Meanwhile, for $N_2/O_2/CH_4$ mixtures, besides NH_3 and traces of HCN, reactions products such as H_2O and CO are formed for O_2 concentrations between 0.3% and 1%. For an oxygen concentration of 3%, CO and H_2O are major products with CO_2 and N_2O appearing in the range of traces. This change in reaction products for relatively high concentration of O_2 can be accounted by assuming that the total oxidation of methane (i.e., a process based on the overall equation $CH_4 + 3/2O_2 \rightarrow CO + 2H_2O$, whereby a minimum of 1.5 molecules of O_2 are required for each of CH_4) is favored with respect to the other reactions involving nitrogen. The most significant difference in comparison with previously reported results with Ar is that neither solid carbon deposits nor higher hydrocarbon species (i.e. C_2H_y) are produced in poor oxygen mixtures. Instead, HCN, NH_3, and H_2O are the main products obtained with N_2 as carrier gas (see Table 3). However, when relatively high concentrations of O_2 are present, the reaction products are similar for both carrier

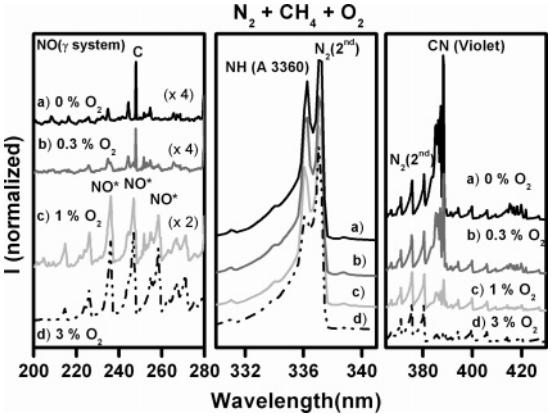

Figure 2. OES spectra for $N_2 + CH_4 + O_2$ mixtures for different concentrations of oxygen at fixed CH_4 values (3000 ppm): (a) $N_2 + CH_4 + O_2$ (0%); (b) $N_2 + CH_4 + O_2$ (0.3%); (c) $N_2 + CH_4 + O_2$ (1%); (d) $N_2 + CH_4 + O_2$ (3%). Left: Bands attributed to NO^* and C^* species. Middle: Bands attributed to N_2^* and NH^* species. Right: Bands attributed to N_2^* and CN^* species.

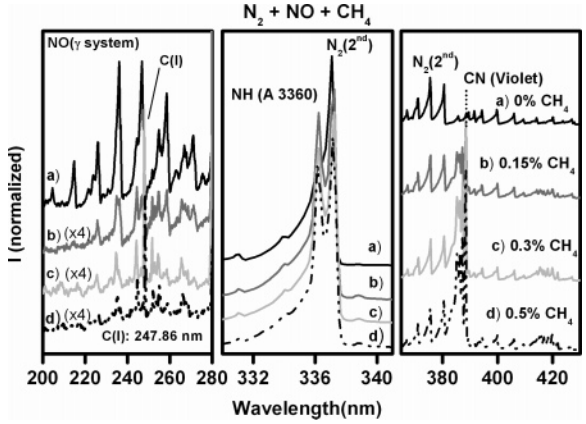

Figure 3. OES spectra for mixtures $N_2 + NO + CH_4$ for different concentrations of CH_4: (a) $N_2/NO/CH_4$ (0%); (b) $N_2/NO/CH_4$ (0.15%); (c) $N_2/NO/CH_4$ (0.3%); (d) $N_2/NO/CH_4$ (0.5%). Left: Bands attributed to NO^* and C^* species. Middle: Bands attributed to N_2^* and NH^* species. Right: Bands attributed to N_2^* and CN^* species.

gases. These products basically result from the partial oxidation of CH_4, HCN, and NH_3.

The OES analysis of the plasma shows the formation of various intermediate species. The spectra collected for different relative concentrations of O_2 are reported in Figure 2. At first sight, the bands due to NO^* increase in intensity, while those due to CN^* diminish as the amount of O_2 in the reaction mixture increases. In comparison with the OES spectra recorded for mixtures $Ar/CH_4/O_2$, an important difference is that bands due to C_2^* species, detected when using Ar as the carrier gas, are not detected in the present case. This fact suggests that C_2^* are intermediate species in the formation of the solid carbon, a majority product obtained with mixtures Ar/CH_4. For mixtures $N_2/CH_4/O_2$ atomic C^* species (see Figure 2 (left)), characterized by a narrow peak at 247.86 nm (see Table 2), NH^* species (peak at 336.0 nm), and CH^* bands in the range of 425−445 nm are the most significant species observed in the spectra of Figure 2. The CN^* species, giving rise to a series of bands at around 388 nm when no oxygen is present in the mixture (red system; see Table 2), proves the relevant role of CN^* intermediate reaction species in the plasma reactions under these lean-O_2 conditions.

The formation of NH_3 as reaction product is indicated by the identification of NH^* intermediate species in the OES spectra (see Figure 2). It is worth noting that the intensity of the corresponding band decreases as the amount of O_2 is enhanced. This fact suggests that active species of nitrogen associate with oxygen instead of H, when O_2 is present in the reaction mixture. In this sense, we observed the existence of atomic lines for N^* (672.09 nm) and H^* (656.28 nm) (see Table 2) which might be directly related to the dissociation of this NH intermediate, since they only appear when CH_4 is introduced in the mixture and there is no relevant emission signal of them in the ternary $N_2/NO/O_2$ mixtures from the previous section. A similar behavior can be observed with regard to C^* and CH^* intermediates, whose intensities decrease as the concentration of oxygen increases (data not shown).

C. Mixtures $N_2/NO/CH_4$. Essays with this mixture were carried out for three different concentrations of CH_4, namely 0.15, 0.30, and 0.50%. These low concentrations of CH_4 have been selected on purpose to check whether the dissociation pattern of CH_4 may be affected by NO. Note in this respect that the reductive power of one molecule of CH_4 is equivalent, at least, to three molecules of NO (i.e., $CH_4 + 3NO \rightarrow 3/2N_2 + 2H_2O + CO$). The results summarized in Table 4 indicates that both reactants, NO and CH_4, are almost completely decomposed by the plasma and that the majority products of this reaction are CO, HCN, and H_2O (H_2). In comparison with the results reported for mixtures $Ar/CH_4/NO$, the main difference resides on the lack of detection of C_2 or higher hydrocarbons.

The OES analysis of the plasma reported in Figure 3 reveals the formation of excited species of N_2^* (second positive system), CN^* (violet and red system), and NH^* (A 3360). CH^* (A 4300 system), N^* (672.09 nm), and H^* (H_α, H_β) intermediates are also detected but not appreciably in the figure (see Table 2). In addition, the narrow peak at 247.86 nm, attributed to C^* atomic species (see Table 2), is also recorded. It has a maximum intensity for a concentration of 0.5% CH_4. It is also noteworthy in this figure that the intensity of the $NO\gamma$ bands decreases while the CN^* bands increase with the concentration of CH_4 in the mixture. Meanwhile, the intensity of the band due to NH^* species remains practically constant, once CH_4 is added, regardless the concentration in the mixture (see Figure 3 (right)).

The reductive effect of CH_4 in the plasma reaction is evidenced in Figure 3 (left) by the decrease of intensity of the NO^* bands as the percentage of methane in the mixture increases. Meanwhile, the formation of HCN is congruent with the monitoring by OES of high-intensity bands due to CN^* intermediates (violet system displayed in Figure 3 (right) and red system not displayed).

D. Mixtures $N_2/NO/O_2/CH_4$. This mixture represents the best approach under our experimental conditions to the composition of real exhausts (note, however, that real exhausts are much more complex with the presence of water vapor, CO_2, soot particles, and eventually higher hydrocarbons). A series of tests

TABLE 4: Reaction Products for $N_2 + NO + CH_4$ Mixtures Containing Different Concentrations of CH_4

reacn mixture	NO removal (%)	CH_4 removal (%)	reacn products (ppm)
$N_2 + NO$	97		N_2, O_2, N_2O (traces)
$N_2 + NO + CH_4$ (0.15%)	100	100	H_2, HCN (<700), CO (<800), NH_3 (<1400), H_2O (<2200)
$N_2 + NO + CH_4$ (0.30%)	100	98	H_2, HCN (<1300), CO (<1700), NH_3 (<1400), H_2O (<1300)
$N_2 + NO + CH_4$ (0.50%)	100	96	H_2, HCN (<3400), CO (<1600), NH_3 (<1300), H_2O (<1400)

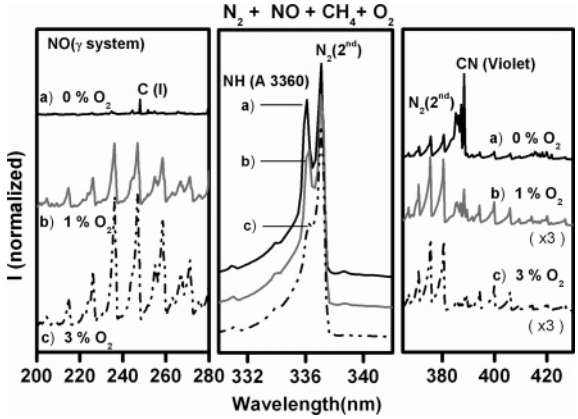

Figure 4. OES spectra for $N_2 + NO + CH_4 + O_2$ mixtures for different concentrations of oxygen at fixed CH_4 values (3000 ppm): (a) $N_2 + NO + CH_4 + O_2$ (0%); (b) $N_2 + NO + CH_4 + O_2$ (1%); (c) $N_2 + NO + CH_4 + O_2$ (3%). Left: Bands attributed to NO^* and C^* species. Middle: Bands attributed to N_2^* and NH^* species. Right: Bands attributed to N_2^* and CN^* species.

have been done by varying the concentration of CH_4 and O_2 in the mixture. A summary of the reaction products detected in each case, as well as efficiency data with respect to the decomposition of NO, is reported in Table 5. In all cases, the majority reaction products were CO and H_2O, while CO_2 and N_2O were detected as traces. On the other hand, while CH_4 decomposes almost completely in all cases, the percentage of decomposition of NO decreases as the amount of oxygen in the mixture increases.

The NO removal efficiency reaches only about 60% for an oxygen concentration of 3%. It is interesting that 100% decomposition is found when the concentration of O_2 is a minimum (i.e., 1%) and that of CH_4 a maximum (i.e., 0.5%)

Figure 4 shows the OES spectra detected for these quaternary mixtures. The detected peaks and bands correspond to N_2^*, NO^*, NH^*, and CN^* excited-state species (Table 2). The addition of higher concentrations of oxygen to the mixture leads to an increase in the number of NO^* species (Figure 4 (left)) and a decrease of that of CN^*, H^*, N^*, C^*, and NH^* intermediates (Figure 4). For greater concentrations of CH_4 (i.e., 0.5%) the same type of bands are detected, although the intensity for the species involving C, N, and /or H atoms increases (effect not shown in the figure). Besides, it must be pointed out the very low intensity of the emission peaks corresponding to atomic H^* (i.e., H_α, H_β, H_γ) and O^* and that of the bands of CH^* (A 4300 system) in most of the OES spectra registered for the N_2 mixtures, especially if compared with the previous experiments carried out in Ar.[15]

IV. Discussion

A first evidence from the previous results is that NO can be effectively removed in a microwave SW cold plasma from a gas mixture with a composition very similar to that of real combustion streams. The fact that, even in the presence of oxygen, the use of N_2 as the carrier gas does not impede the decomposition of NO opens interesting questions regarding the plasma decomposition mechanisms. The explanation of the removal of NO and the induction of other secondary reactions depending on the gas mixtures requires a careful assessment of the possible reaction pathways for each particular gas composition. In the following we will discuss the possible reaction processes occurring for the different mixtures in relation with previously published data for plasma reactions with more simple gas mixtures.[5,6,13,21,24,29,30,34−36]

A. Mixtures N_2/NO and N_2/NO/O_2. NO is efficiently converted into N_2 and O_2 when nitrogen is used as carrier gas. According to the known reactions taking place in nitrogen plasmas, ground-state $N(^4S)$ species formed by plasma decomposition of nitrogen[4,27,36] can effectively lead to the decomposition of the small amounts of NO existing in our gas mixture. Another alternative would be the involvement of $N(^2D)$ excited atoms, although many authors consider that they are rapidly converted to NO in the presence of oxygen.[24,36] Therefore, the most likely reaction process would be

$$N(^4S) + NO(X) \rightarrow N_2(X,v) + O \qquad k_1 = 3.0 \times 10^{-11}\ \mathrm{cm^3/s},\ T = 298\ \mathrm{K}\ ^{37} \quad (1)$$

$$N(^2D) + NO(X) \rightarrow N_2(X,v) + O \qquad k_2 = 4.5 \times 10^{-11}\ \mathrm{cm^3/s},\ T = 298\ \mathrm{K}\ ^{37} \quad (2)$$

where NO(X) are ground-state molecules of this gas. The formation of atomic species of nitrogen in a SW plasma of nitrogen may proceed according to a large variety of processes as it is reported in Table 6. This table summarizes a series of plasma reactions taken from the literature and can be of importance to account for the results found in our experiments. Reactions T1 and T2, where electron impact processes are involved, can be an effective source of $N(^4S)$ and $N(^2D)$ atomic species and also of molecular metastable $N_2(A^3\Sigma_u^+)$ states. These species may transfer their energy to other species present in the discharge[24,27] (e.g., see reaction T4).

N_2O in the range of traces has been detected as byproduct of the plasma reaction (cf., Table 1). Its formation very likely involves O atoms, as those produced through reaction 1 or reaction T4, this latter involving $N_2(A)$ excited molecules. These atomic oxygen species may then react according to

$$O + NO \rightarrow NO_2 \qquad k_3 = 3.0 \times 10^{-11}\ \mathrm{cm^3/s},\ T = 200{-}1500\ \mathrm{K}\ ^{34} \quad (3)$$

$$N + NO_2 \rightarrow N_2O + O \qquad k_4 = 3.0 \times 10^{-12}\ \mathrm{cm^3/s},\ T = 298\ \mathrm{K}\ ^{38} \quad (4)$$

with N_2O as a final reaction product.

In the presence of oxygen, the decomposition yield of NO decreases. This result is a consequence of the fact that oxygen produces a decrease in the electron temperature, thus making reactions less effective (eqs T1, T2). In addition, the production of some NO in parallel to its decomposition is another expected effect of the presence of oxygen in the plasma gas. These two effects are consistent with the small dissociation energy of O_2 as compared to that of N_2 and with the expected increase in the concentration of atomic oxygen as the O_2 in the mixture increases. In fact, atomic oxygen (O), either in the $O(^3P)$ or $O(^1D)$ states, can be effectively produced through reaction T3. Under these conditions, NO can be produced by collision of O or N atoms with N_2 and O_2 molecules as shown in reactions 5−8:

$$N_2(X, v > 13) + O \rightarrow NO + N(^4S) \qquad k_5 = 1.0 \times 10^{-13}\ \mathrm{cm^3/s},\ T = 298\ \mathrm{K}\ ^{24} \quad (5)$$

$$N_2(A) + O \rightarrow NO + N(^2D) \qquad k_6 = 7.0 \times 10^{-12}\ \mathrm{cm^3/s},\ T = 298\ \mathrm{K}\ ^{36} \quad (6)$$

$$N(^2D) + O_2 \rightarrow NO + O$$
$$k_7 = 4.5 \times 10^{-11}\ cm^3/s,\ T = 298\ K\ ^{39} \quad (7)$$

$$N(^4S) + O_2 \rightarrow NO + O$$
$$k_8 = 3.6 \times 10^{-15}\ cm^3/s,\ T = 280-910\ K\ ^{40} \quad (8)$$

Reaction 5 may occur in discharges where N_2 molecules present a vibrational distribution characterized by the population of vibrational quantum numbers greater than 12.[23,24] Reaction 6 requires metastable states of the N_2 molecule which may also participate in the NO excitation processes (e.g., reaction T4). On the other hand, reactions 7 and 8 can be rather effective in producing NO if the amount of atomic nitrogen is high.[41] The activity of N atoms in producing NO was confirmed in previous experiments of our group where significant amounts of NO were produced in a SW plasma with Ar as carrier gas and N_2 and O_2 in small concentrations.[15]

Therefore, through reactions T3 and/or 4−8, the participation of oxygen will be a critical factor contributing to the decrease in the overall yield of NO decomposition in mixtures N_2/NO/O_2. An additional reaction pathway leading to the formation of NO is a wall process involving single N and O atoms at the wall of the discharge tube (i.e., N + O (wall) → NO (wall)).[42]

The previous plasma reaction scheme is supported by OES observations. Thus, for the mixture N_2/NO, we have detected the NOγ system bands (230−290 nm) emitted by the excited state NO(A) (i.e., corresponding to the NO(A) → NO(X) + $h\nu$ deexcitation), this latter very likely produced through reaction T4. By contrast, the NOβ system bands (250−320 nm), emitted by NO(B) excited molecules,[25] are not detected in our system. This indicates that the concentration of NO(B) excited molecules, formed through a three-body reaction involving the combination of N(^{4}S) and O atoms in the presence of N_2 or O_2, is negligible in our system.[24] The other spectral bands recorded under these conditions are the nitrogen first positive system (i.e., corresponding to the transition $N_2(B^3) \rightarrow N_2(A^3) + h\nu$) and the nitrogen second positive system (i.e., $N_2(C^3) \rightarrow N_2(B^3) + h\nu$). Note that $N_2(A^3)$ and $N_2(B^3)$ species are involved in reaction T5, which is very effective at pressures of the order of that used in our experiment.

In mixtures N_2/NO/O_2, the increase of the intensity of NO* bands with the concentration of oxygen in the plasma (cf. Figures 1, 2, and 4) is also in agreement with the previous reaction scheme. This observation supports an enhancement of the concentration of NO(A) excited species, even though reactions such as T6−T8 might simultaneously contribute to quench these states by reaction with N_2, O_2, or NO.[24]

In summary, the increase of the concentration of oxygen favors the formation of NO, detected in the NOγ system (see Figure 1). Despite of the expected active role of the atomic N and O species, its rapid recombination does not permit its identification by OES, if compared with other carrier gases or experimental setups.[13,15,18] Nevertheless, some authors propose a titration method by adding Ar−NO mixtures to determine the density of atomic species from molecular bands,[28,43−45] although these measurements have not been carried out in this work due to the lack of N_2 pure discharge experiments.

B. N_2/NO/CH_4. The use of hydrocarbons as reductant compounds to improve the removal efficiency of NO_x has been extensively studied both theoretically and experimentally.[1,16,32,46−48] When CH_4 is added to the N_2/NO mixture, NO is very effectively removed and new intermediate species can be detected by OES (Figure 2 (left)). The most remarkable intermediate corresponds to CN* radicals giving rise to the bands of the violet and red emission systems (Table 2). These bands become more intense as the CH_4 content in the mixture increases (Figure 2 (right)). Moreover, NH* intermediates can be also recognized when methane is added to the gas mixture (see Figure 2 (center)). According to previous works in the literature,[30] the addition of CH_4 must contribute to the decrease in the concentrations of N_2(B) and N_2(C) states, responsible for the emission of the first and second positive systems of N_2^*, as well as for generation of N(^{4}S) atoms. A similar behavior is also expected in our system. A possible reaction by which a low concentration of CH_4 in the mixture would produce a sharp decrease in the concentration of N atoms is their direct reaction with CH_x radicals produced by electron collisions with CH_4:[24,41,49]

$$N + CH_x \rightarrow CN + xH \quad (9)$$

$$2CH_4 + N \rightarrow CH + CN + 3H_2 + H \quad (10)$$

In comparison with our previous results using Ar as carrier gas,[15] reactions 9 and 10 can also explain the depletion of C_2H_y and CH* excited species (A 4300 system) observed respectively by MS and OES. Additional reaction pathways for the formation of C atoms and subsequently CN species are proposed in reactions T9 and T10. In contrast to previous experiments in Ar,[15,50] there is a manifest absence of deposits of carbon and C_2^* intermediate species when N_2 is used as the carrier gas. This fact is in part attributed to the presence of active N atoms in the nitrogen plasma and to the high activity of these species for the removal of carbon through its transformation into CN species.

The CN* radicals detected by OES must be the precursor species for the formation of the stable HCN, subsequently detected by MS (Table 3). Different routes are proposed by computational and experimental methods to account for the formation of this noxious product.[24,51] Some of the possible reactions involved are reported in Table 6 (reactions T11−T13).

Meanwhile, the simultaneous observation by OES and MS of NH* species in the plasma and NH_3 as a final product (cf., Tables 2 and 3) can be accounted for by a combination of reactions T13−T18 and T23. In turn, the formed NH* radicals can also participate actively in the formation and removal processes of NO, according to reactions T19−T22. The presence of N* and H* atomic lines (see Table 2) previously pointed out in the section IIIB might be indeed related to the direct dissociation and/or formation of NH*, since its intensities increase with the methane content (reaction T16). Concerning the atomic density of N, no quantitative data can be provided although we can assume qualitatively that the intensity of the band at 580.4 nm, used by Ricard et al.,[28,43−45] diminishes if compared with the N_2/NO/O_2 mixtures, which means that our system behaves in a way similar to that previously described in the literature.[28,43−45]

CO is another product detected by MS with the mixtures containing methane. The formation of this product should proceed by the reaction of O atoms dissociated from NO with other active species containing carbon such as CN and/or CH_x:

$$CN + O \rightarrow CO + N(^4S, ^2D)$$
$$k_{11} = 1.7 \times 10^{-11}\ cm^3/s,\ T = 300-5000\ K\ ^{29} \quad (11)$$

$$O + CH \rightarrow CO + H$$
$$k_{12} = 6.6 \times 10^{-11}\ cm^3/s,\ T = 300-2500\ K\ ^{29} \quad (12)$$

TABLE 5: Reaction Products for $N_2 + NO + CH_4 + O_2$ Mixtures Containing Different Concentrations of CH_4 and O_2

reacn mixture	NO removal (%)	CH_4 removal (%)	O_2 conversn (%)	reacn products (ppm)
$N_2 + NO + CH_4$ (0.3%) + O_2 (1%)	90	97	42	H_2, CO (<2300), NH_3, H_2O (<8000), CO_2 (<500), N_2O (traces)
$N_2 + NO + CH_4$ (0.3%) + O_2 (3%)	67	97	14	H_2, CO (<2000), NH_3, H_2O (<6500), NO (<1000), CO_2 (<400), N_2O (traces)
$N_2 + NO + CH_4$ (0.5%) + O_2 (1%)	100	100	78	H_2, CO (<3800), NH_3, H_2O (<6500), CO_2 (<600), N_2O (traces)
$N_2 + NO + CH_4$ (0.5%) + O_2 (3%)	60	100	23	H_2, CO (<3900), NH_3, H_2O (<8400), CO_2 (<700), NO (<1200)

TABLE 6: Summary of Plasma Reactions Induced by MW Discharges That Can Be Involved in the Decomposition Processes Observed in This Work

no.[a]	reacns	rate constants k_{298} (cm^3 $molecule^{-1}$ s^{-1})	temp range (K)	refs
T1	$e + N_2(X) \rightarrow e + N(^4S) + N(^4S,^2D)$	f (E/N)		52
T2	$e + N_2(X) \rightarrow e + N_2(A)$	f (E/N)		40
T3	$e + O_2 \rightarrow e + O(^3P) + O(^3P,^1D)$	f (E/N)		53
T4	$N_2(A) + NO(X) \rightarrow N_2(X) + NO(A)$	6.4×10^{-11}		54
T5	$N_2(X,v) + N_2(A) \rightarrow N_2(X) + N_2(B,v)$	2.0×10^{-11}		54
T6	$NO(A) + N_2 \rightarrow NO(X) + N_2$	1.0×10^{-13}		24
T7	$NO(A) + O_2 \rightarrow NO(X) + O_2$	1.5×10^{-10}		24
T8	$NO(A) + NO \rightarrow NO(X) + NO$	1.0×10^{-10}		24
T9	$N + CN \rightarrow C + N_2$	6.6×10^{-11}		42
T10	$C + N + N_2 \rightarrow CN(B,7) + N_2$	1.5×10^{-13}		42
T11	$CN + H_2 \rightarrow HCN + H$	1.5×10^{-13}		30
T12	$CN + CH_4 \rightarrow HCN + CH_3$	3.4×10^{-10}		30
T13	$N + H_2CN \rightarrow HCN + NH$	6.7×10^{-11}		30
T14	$NO + H \rightarrow HNO$	2.5×10^{-10}	300	55
T15	$H + HNO \rightarrow OH + NH$	2.4×10^{-9}	313	56
T16	$N_2(A) + H \rightarrow NH + N$	2.1×10^{-10}		57
T17	$N(^2D) + H_2O \rightarrow NH + OH$	2.5×10^{-10}	200−300	39
T18	$N(^2D) + H_2 \rightarrow NH(X) + H$	2.3×10^{-12}	200−300	58
T19	$NH + NO \rightarrow N_2O + H$	5×10^{-11}	270−380	29
T20	$NH + NO \rightarrow N_2 + OH$	5×10^{-11}	270−380	29
T21	$NH + OH \rightarrow NO + H_2$	8.0×10^{-11}	300−1000	29
T22	$NH + O \rightarrow NO + H$	6.6×10^{-11}		29
T23	$CN + OH \rightarrow CO + NH$	1.4×10^{-10}	292	59
T24	$CN + O_2 \rightarrow CO + NO$	6.1×10^{-12}	292	59
T25	$CN + O_2 \rightarrow NCO + O$	2.2×10^{-11}	300−2500	29
T26	$NCO + NO \rightarrow N_2O + CO$	3.3×10^{-11}	500−3000	29
T27	$NCO + NO \rightarrow N_2 + CO_2$	3.3×10^{-11}	500−3000	29
T28	$NCO + NO \rightarrow N_2 + CO + O$	3.3×10^{-11}	500−3000	29
T29	$H + CHO \rightarrow H_2 + CO$	1.5×10^{-10}	300−2500	29
T30	$CO_2 + CH \rightarrow H + 2CO$	1.8×10^{-12}	300−1000	29
T31	$CO_2 + N_2(A) \rightarrow N_2 + CO + O$	7.2×10^{-13}		39
T32	$CO_2 + N(^2D) \rightarrow CO + NO$	1.3×10^{-11}		39

[a] T1−T3: Electron impact dissociation processes. Coefficients are dependent on E/N values and electron energy distribution function (EEDF). T4: Only mechanism responsible for the NO(A) excited states production. T6−T8: Quenching processes of NO(A) species. T9−T13 and T23−T28: Kinetics involving CN^* and HCN^* species. T13−T23: Reactions for NH^* intermediates. T23−T32: Processes related with CO^* production. T31−T32: Reactions responsible for CO_2 back-reduction to CO.

Owing to the long average lifetime of CN^* species,[30] the most likely reaction is one that involves these intermediates (i.e., reaction 11). In this way, CN^* might also be a possible source of $N(^4S)$ excited states very active for the decomposition of NO (reaction 1).

In summary, the presence of increasing amounts of CH_4, beyond the further decomposition of NO, is favoring the formation of CN^* and NH^* intermediates, which might be also responsible of the raising presence of N and H atomic species, detected by OES, through reactions T11 and T16. Additionally, the formation of CO as product is determined by MS but not observed in the emission spectra and may occur through reactions 11 and 12 and T23 and T24.

C. $N_2/NO/CH_4/O_2$. A first glance to the results obtained with this mixture evidence that they are the convolution of those obtained for the $N_2/NO/CH_4$, $N_2/CH_4/O_2$, and $N_2/NO/O_2$ mixtures. Other evidence is that the concentration of the different minority components (i.e., CH_4 and O_2) is the key parameter for the control of the final removal efficiency of NO and the definition of the other byproducts formed in the reaction processes. Thus, when the relative concentrations of O_2 and CH_4 are 1% and 0.5%, practically 100% decomposition of NO is obtained. When the concentration of oxygen increases up to 3%, NO removal efficiency decreases down to 60%. From a practical point of view this might indicate that the solution for an effective NO removal would be to decrease the oxygen content in the mixture. However, this type of adjustments should be handled very carefully since HCN, a compound more noxious than NO, can then be formed in mixtures with little oxygen (cf. Table 4). It is also worth mentioning that in the present experiment, contrary to other plasma processes based on DBD discharges where NO_2 is formed,[5,6] only decomposition into N_2 and O_2 is found.

In mixtures N_2 (carrier) + NO + CH_4 + O_2, the actual O_2/CH_4 ratio in the gas mixture is a critical parameter not only for the control of the final product composition but also for the determination of the intensity of the different bands monitored by OES. Thus, in comparison with the behavior observed for the $N_2/NO/CH_4$ mixture, the presence of O_2 seems to favor the oxidation of the intermediate species formed out of CH_4 (i.e., CN, CH, and NH) toward CO, CO_2, and H_2O as final products (cf., Figure 4 (center and right)). Reactions T23−T32 are

proposed as possible additional processes occurring under our conditions to account for the evolution of reaction products reported in Table 5 and the evolution of the OES spectra in Figure 4. The atomic N and H species detected (see Table 2) respond in an way opposite to the increment of the oxygen percentage, since the intensity of the former decreases while the intensity of the latter increases. This fact again might be correlated with processes where NH intermediates intervene and reactions T16 and T22 are favored.

In conclusion, the experimental conditions described in the ternary mixtures are also reproduced in the quaternary ones. In these mixtures, oxygen is always present and that means that the intensity of CN, NH, and CH is reduced to minimum traces (Table 5), while the percentage of decomposition of NO is not so favored (see reactions 4−8). The same tendencies as in the ternary mixtures can be observed for the N and H atomic species, since the intensity of the former decreases and that of the latter increases, when the amount of oxygen is enhanced (reactions T16 and T22 in Table 6).

V. Conclusions

The previous results and discussion have shown that NO can be efficiently removed by flowing plasmas from complex gas mixtures containing nitrogen as carrier gas and oxygen and hydrocarbons as minority components. The plasma processes involved in the reactions are very complex, and a precise control of the component gases is required if plasma abatement is to be used for practical NO removal. In fact, while increasing the oxygen concentration may prevent the formation of unwanted byproducts such as HCN or NH_3, a too high concentration of this gas (i.e., >3%) may drastically reduce the removal efficiency of NO. This implies that an effective use of flowing plasma processes for the removal of noxious gases requires a very strict control of the gas composition within very narrow margin of concentrations.

The observations made by OES and MS of respectively given intermediate species in the plasma and final reaction products have been rationalized by considering the information existing in the literature about elemental plasma reactions. However, a more detailed description of the reaction mechanisms involved with these complex plasma mixtures still requires more precise kinetic models accounting for all the meaningful parameters of the plasma discharge (i.e., actual temperature of species, effects of gases adsorbed in the walls, etc.).

Acknowledgment. We thank the Ministry of Education and Science of Spain for financial support (Project Nos. PPQ2001-3108 and ENE2004-01660 and a Ph.D. grant).

References and Notes

(1) Rajanikanth, B. S.; Srinivasan, A. D.; Ravi, V. *IEEE Trans. Dielectr. Electr. Insul.* **2005**, *12*, 72.

(2) Penetrante, B. M.; Hsiao, M. C.; Merritt, B. T.; Vogtlin, G. E.; Wallman, P. H.; Neiger, M.; Wolf, O.; Hammer, T.; Broer, S. *Appl. Phys. Lett.* **1996**, *68*, 3719.

(3) Chae, J. O. *J. Electrost.* **2003**, *57*, 251.

(4) Penetrante, B. M.; Brusasco, R. M.; Merritt, B. T.; Vogtlin, G. E. *Pure Appl. Chem.* **1999**, *71*, 1829.

(5) Penetrante, B. M.; Hsiao, M. C.; Merritt, B. T.; Vogtlin, G. E.; Wallman, P. H.; Kuthi, A.; Burkhart, C. P.; Bayless, J. R. *Appl. Phys. Lett.* **1995**, *67*, 3096.

(6) Dorai, R.; Kushner, M. J. *J. Phys. D: Appl. Phys.* **2001**, *34*, 574.

(7) Mok, Y. S.; Ham, S. W. *Chem. Eng. Sci.* **1998**, *53*, 1667.

(8) Rajanikanth, B. S.; Ravi, V. *Plasma Sci. Technol.* **2004**, *6*, 2411.

(9) Hu, X. D.; Zhang, J. J.; Mukhnahallipatna, S.; Hamann, J.; Biggs, M. J.; Agarwal, P. *Fuel* **2003**, *82*, 1675.

(10) Timmermans, E. A. H.; Jonkers, J.; Rodero, A.; Quintero, M. C.; Sola, A.; Gamero, A.; Schram, D. C.; van der Mullen, J. A. M. *Spectrochim. Acta, Part B* **1999**, *54*, 1085.

(11) Baeva, M.; Gier, H.; Pott, A.; Uhlenbusch, J.; Hoschele, J.; Steinwandel, J. *Plasma Chem. Plasma Process.* **2001**, *21*, 225.

(12) Al-Shamma's, A. I.; Wylie, S. R.; Lucas, J.; Pau, C. F. *J. Phys. D: Appl. Phys.* **2001**, *34*, 2734.

(13) Luo, J.; Suib, S. L.; Marquez, M.; Hayashi, Y.; Matsumoto, H. *J. Phys. Chem. A* **1998**, *102*, 7954.

(14) Castillo, M.; Herrero, V. J.; Tanarro, I. *Plasma Sources Sci. Technol.* **2002**, *11*, 368.

(15) Hueso, J. L.; González-Elipe, A. R.; Cotrino, J.; Caballero, A. *J. Phys. Chem. A* **2005**, *109*, 4930.

(16) Zhu, A. M.; Sun, Q.; Niu, J. H.; Xu, Y.; Song, Z. M. *Plasma Chem. Plasma Process.* **2005**, *25*, 371.

(17) Penetrante, B. M.; Hsiao, M. C.; Merritt, B. T.; Vogtlin, G. E.; Wallman, P. H. *IEEE Trans. Plasma Sci.* **1995**, *23*, 679.

(18) Luo, J.; Suib, S. L.; Hayashi, Y.; Matsumoto, H. *J. Phys. Chem. A* **1999**, *103*, 6151.

(19) Chae, J. O.; Hwang, J. W.; Jung, J. Y.; Han, J. H.; Hwang, H. J.; Kim, S.; Demidiouk, V. I. *Phys. Plasmas* **2001**, *8*, 1403.

(20) Rajanikanth, B. S.; Das, S.; Srinivasan, A. D. *Plasma Sci. Technol.* **2004**, *6*, 2475.

(21) Gentile, A. C.; Kushner, M. J. *J. Appl. Phys.* **1995**, *78*, 2074.

(22) Dorai, R.; Kushner, M. J. *J. Phys. D: Appl. Phys.* **2002**, *35*, 2954.

(23) Gordiets, B. F.; Ferreira, C. M.; Guerra, V. L.; Loureiro, J.; Nahorny, J.; Pagnon, D.; Touzeau, M.; Vialle, M. *IEEE Trans. Plasma Sci.* **1995**, *23*, 750.

(24) Pintassilgo, C. D.; Loureiro, J.; Guerra, V. *J. Phys. D: Appl. Phys.* **2005**, *38*, 417.

(25) Pointu, A. M.; Ricard, A.; Dodet, N.; Odic, E.; Larbre, J.; Ganciu, M. *J. Phys. D: Appl. Phys.* **2005**, *38*, 1905.

(26) Henriques, J.; Villeger, S.; Levaton, J.; Nagai, J.; Santana, S.; Amorim, J.; Ricard, A. *Surf. Coat. Technol.* **2005**, *200*, 814.

(27) Guerra, V.; Galiaskarov, E.; Loureiro, J. *Chem. Phys. Lett.* **2003**, *371*, 576.

(28) Diamy, A. M.; Hochard, L.; Legrand, J. C.; Ricard, A. *Surf. Coat. Technol.* **1998**, *98*, 1377.

(29) Baulch, D. L.; Cobos, C. J.; Cox, R. A.; Esser, C.; Frank, P.; Just, T.; Kerr, J. A.; Pilling, M. J.; Troe, J.; Walker, R. W.; Warnatz, J. *J. Phys. Chem. Ref. Data* **1992**, *21*, 411.

(30) Pintassilgo, C. D.; Loureiro, J.; Cernogora, G.; Touzeau, M. *Plasma Sources Sci. Technol.* **1999**, *8*, 463.

(31) Savinov, S. Y.; Lee, H.; Song, H. K.; Na, B. K. *Plasma Chem. Plasma Process.* **2003**, *23*, 159.

(32) Bromly, J. H.; Barnes, F. J.; Muris, S.; You, X.; Haynes, B. S. *Combust. Sci. Technol.* **1996**, *115*, 259.

(33) Pearse, R. W. B.; Gaydon, A. G. In *The Identification of Molecular Spectra*; Champan and Hall: New York, 1976.

(34) Atkinson, R.; Baulch, D. L.; Cox, R. A.; Hampson, R. F.; Kerr, J. A.; Troe, J. *J. Phys. Chem. Ref. Data* **1989**, *18*, 881.

(35) Atkinson, R.; Baulch, D. L.; Cox, R. A.; Hampson, R. F.; Kerr, J. A.; Rossi, M. J.; Troe, J. *J. Phys. Chem. Ref. Data* **1997**, *26*, 1329.

(36) Kossyi, I. A.; Kostinsky, A. Y.; Matveyev, A. A.; Silakov, V. P. *Plasma Sources Sci. Technol.* **1992**, *1*, 207.

(37) Herron, J. T.; Green, D. S. *Plasma Chem. Plasma Process.* **2001**, *21*, 459.

(38) Atkinson, R.; Baulch, D. L.; Cox, R. A.; Hampson, R. F.; Kerr, J. A.; Troe, J. *J. Phys. Chem. Ref. Data* **1992**, *21*, 1125.

(39) Herron, J. T. *J. Phys. Chem. Ref. Data* **1999**, *28*, 1453.

(40) Fernandez, A.; Goumri, A.; Fontijn, A. *J. Phys. Chem. A* **1998**, *102*, 168.

(41) Ricard, A.; Jaoul, C.; Gaboriau, F.; Gherardi, N.; Villeger, S. *Surf. Coat. Technol.* **2004**, *188−189*, 287.

(42) Pintassilgo, C. D.; Cernogora, G.; Loureiro, J. *Plasma Sources Sci. Technol.* **2001**, *10*, 147.

(43) Diamy, A. M.; Hochard, L.; Legrand, J. C.; Ricard, A. *Plasma Chem. Plasma Process.* **1998**, *18*, 447.

(44) Diamy, A. M.; Legrand, J. C.; Moritts, A.; Ricard, A. *Surf. Coat. Technol.* **1999**, *112*, 38.

(45) Jaoul, C.; Czerwiec, T.; Belmonte, T.; Ricard, A.; Michel, H. *Eur. Phys. J.: Appl. Phys* **2004**, *26*, 227.

(46) Orlandini, I.; Riedel, U. *J. Phys. D: Appl. Phys.* **2000**, *33*, 2467.

(47) Dorai, R.; Kushner, M. J. *J. Appl. Phys.* **2000**, *88*, 3739.

(48) Niessen, W.; Wolf, O.; Schruft, R.; Neiger, M. *J. Phys. D: Appl. Phys.* **1998**, *31*, 542.

(49) Pereira, J.; Massereau-Guilbaud, V.; Geraud-Grenier, I.; Plain, A. *Plasma Process. Polym.* **2005**, *2*, 633.

(50) Heintze, M.; Magureanu, M.; Kettlitz, M. *J. Appl. Phys.* **2002**, *92*, 7022.

(51) Andersson, S.; Markovic, N.; Nyman, G. *J. Phys. Chem. A* **2003**, *107*, 5439.

(52) Cosby, P. C. *J. Chem. Phys.* **1993**, *98*, 9544.

(53) Cosby, P. C. *J. Chem. Phys.* **1993**, *98*, 9560.
(54) Guerra, V.; Sa, P. A.; Loureiro, J. *J. Phys. D: Appl. Phys.* **2001**, *34*, 1745.
(55) Cohen, N.; Westberg, K. R. *J. Phys. Chem. Ref. Data* **1991**, *20*, 1211.
(56) Forte, E. N. *J. Photochem.* **1981**, *17*, 13.
(57) Ho, G. H.; Golde, M. F. *J. Chem. Phys.* **1991**, *95*, 8866.
(58) Dodd, J. A.; Lipson, S. J.; Flanagan, D. J.; Blumberg, W. A. M.; Person, J. C.; Green, B. D. *J. Chem. Phys.* **1991**, *94*, 4301.
(59) Decker, B. K.; Macdonald, R. G. *J. Phys. Chem. A* **2003**, *107*, 9137.